Available online at www.sciencedirect.com
ScienceDirect
Trans. Nonferrous Met. Soc. China 34(2024) 681−693
Transactions of Nonferrous Metals Society of China
www.tnmsc.cn

Preparation of ultralow-oxygen titanium by direct reduction of TiO_2

Jian PANG[1,2,3], Ling-xin KONG[1,2,3,4], Li-guo ZHU[1,2,3],
Bao-qiang XU[1,2,3,4], Jun-jie XU[1,2,3], Chong-lin BAI[1,2,3], Bin YANG[1,2,3,4]

1. Key Laboratory for Nonferrous Vacuum Metallurgy of Yunnan Province, Kunming University of Science and Technology, Kunming 650093, China;
2. National Engineering Research Center of Vacuum Metallurgy, Kunming University of Science and Technology, Kunming 650093, China;
3. Faculty of Metallurgical and Energy Engineering, Kunming University of Science and Technology, Kunming 650093, China;
4. State Key Laboratory of Complex Non-ferrous Metal Resources Clean Utilization, Kunming University of Science and Technology, Kunming 650093, China

Received 9 September 2022; accepted 14 March 2023

Abstract: A new method for the preparation of low oxygen titanium was proposed by the direct reduction of TiO_2 with Mg produced by $MgCl_2$−KCl−YCl_3 molten salt electrolysis. The Mg−Ti−O phase diagram indicates that it is feasible to reduce TiO_2 using Mg, and the φ−$p_{O^{2-}}$ diagrams indicate that deep deoxidation of titanium in molten $MgCl_2$−YCl_3 is also feasible. The experimental study on the reduction of TiO_2 was carried out in $MgCl_2$−YCl_3 and $MgCl_2$−YCl_3−KCl molten salts. The results showed that the O^{2-} from the reduction and deoxygenation was removed using YOCl precipitation and CO_x gas production and TiO_2 can be reduced to titanium peroxide (Ti_6O) by electrochemical reduction at 1073−1173 K and 2.5−3.1 V. The high-oxygen titanium was electrochemically deoxidized in the molten salt of $MgCl_2$−YCl_3 at a temperature of 1173 K at different voltages. Moreover, it was observed that it is possible to reduce the high oxygen content of titanium from 1200×10^{-6} to less than 100×10^{-6} oxygen.

Key words: titanium dioxide; electrochemistry; magnesium reduction; deoxidation; ultralow-oxygen Ti; rare earth metals

1 Introduction

Titanium (Ti) is an important industrial metal, along with steel and aluminum, with excellent properties such as its light weight, strong corrosion resistance, high specific strength, high heat resistance, and biocompatibility [1−6]. The use of Ti alloys in aircraft manufacturing has rapidly increased. For example, the utilization rate in the manufacturing of Boeing 787 and Airbus A350 aircrafts has increased to approximately 14% in recent years [7,8]. In addition, the global Ti demand for liquefied natural gas transport ships is expected to reach 248000 t by 2030 [9]. However, the global production of Ti was less than 227279 t in 2021, and the disparity between supply and demand has become increasingly apparent [10].

Currently, Ti sponge is predominantly produced by the Kroll process [11,12]. Although this process can produce low-oxygen Ti, its widespread use is limited because of its long processing time, intermittent production, and low efficiency. Therefore, research worldwide is focused on developing low-cost processes for Ti production. The direct production of Ti using TiO_2

Corresponding author: Ling-xin KONG, Tel: +86-15987180307, E-mail: kkmust@126.com;
Bin YANG, Tel: +86-871-65161583, E-mail: kgyb2005@126.com
DOI: 10.1016/S1003-6326(23)66427-1

as raw material, can significantly reduce the process flow and production cost. The most widely used methods for the direct reduction of TiO_2 were studied [13−15], and solid oxide membrane process and electroslag remelting methods were reported [16,17]. However, these methods exhibit low efficiencies, a high oxygen content in the products, and severe iron and carbon pollution.

Oxygen is an undesirable impurity in Ti materials and significantly affects their mechanical properties, especially fracture toughness and fatigue [18]. Various direct methods for the deoxidation of Ti powder or scrap have been reported [19−21]. The most effective method is electrochemical deoxidation in a $CaCl_2$ flux proposed by OKABE et al [22]. With a pure $MgCl_2$ flux at 1173 K, TANINOUCHI et al [23], OKABE et al [24] and ZHENG et al [25] used electrochemically generated magnesium as a deoxidizer to reduce the oxygen content of pure Ti from $(500−1200)\times10^{-6}$. Because the production of Mg is more economical than that of Ca, Mg may be the preferred deoxidizer to remove solid-dissolved oxygen from Ti waste. At present, the electrolytic Mg thermal reduction of titanium dioxide to prepare ultralow-oxygen metallic Ti in $MgCl_2$−YCl_3 and $MgCl_2$−YCl_3−KCl molten salts has not been reported.

This study proposes a new method for preparing ultralow-oxygen Ti via the direct reduction of TiO_2 to address the issues mentioned above. The mechanisms of molten salt electrolysis and magnetocaloric reduction of TiO_2 are presented as follows: First, Ti with a high oxygen content was obtained, and then electrochemically deoxidized to yield Ti with an ultralow oxygen content less than 100×10^{-6}. This novel method of Ti production via the direct reduction of Ti dioxide offers new applications for rare earth metals.

2 Thermodynamic analysis

The standard Gibbs free energy and other thermodynamic data of the Ti−O−Mg system have been reported [26]. A two-parameter model commonly used in thermodynamic calculations and the homologous linear law, were applied to obtaining the standard Gibbs energy of formation (ΔG_f^Θ) for relevant compounds; reliable thermodynamic data were obtained, as shown in Tables 1 and 2. Figure 1 shows that the ternary phase diagram of the Ti−O−Mg system was drawn at 1173 K based on two factors: (1) the ΔG_f^Θ values of the compounds in Table 1, and (2) the standard Gibbs free energy of reaction (ΔG_r^Θ) of the compounds in the Mg−Ti−O system in Table 2.

Figure 1 shows the Mg(l)/MgO(s)/Ti(s) three-phase equilibrium point, which is stable at 1173 K.

Table 1 Standard Gibbs energy of formation of relevant compounds

Compound	ΔG_f^Θ/(J·mol^{-1})	T/K	ΔG_f^Θ(1173 K)/(J·mol^{-1})
MgO (s)	$\Delta G_f^\Theta=-608700+115.9T$	1100−1300	−472750
TiO (s)	$\Delta G_f^\Theta=-532900+87.8T$	1100−1300	−429910
TiO_2 (s)	$\Delta G_f^\Theta=-939800+177.2T$	1100−1300	−731940
Ti_2O_3 (s)	$\Delta G_f^\Theta=-1496000+255.7T$	1100−1300	−1196060
Ti_3O_5 (s)	$\Delta G_f^\Theta=-2428000+417.2T$	1100−1300	−1938620
Ti_4O_7 (s)	$\Delta G_f^\Theta=-3373000+595.6T$	1100−1300	−2674360

Table 2 Standard Gibbs free energy of reaction for relevant compounds in Mg−Ti−O system

Compound	ΔG_r^Θ/(J·mol^{-1})	T/K	ΔG_r^Θ(1173 K)/(J·mol^{-1})
$MgTiO_3$ (s)	MgO (s)+TiO_2(s)=$MgTiO_3$ (s) $\Delta G_r^\Theta=-24780+0.68T$	1173−1361	−23980
$MgTi_2O_5$ (s)	MgO (s)+2TiO_2 (s)=$MgTi_2O_5$ (s) $\Delta G_r^\Theta=-17880-7.75T$	1173−1361	−26970
Mg_2TiO_4 (s)	2MgO (s)+TiO_2 (s)=Mg_2TiO_4 (s) $\Delta G_r^\Theta=-15370-12.20T$	1173−1361	−29680

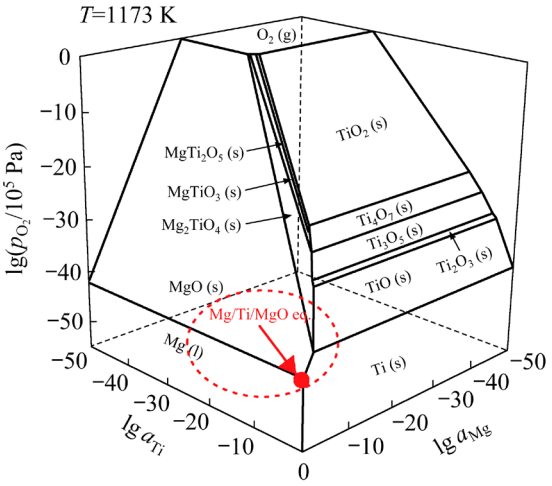

Fig. 1 Phase diagram of Ti−O−Mg ternary system at 1173 K (p_{O_2}–Oxygen partial pressure; a−Activity)

The reduction of TiO_2 by Mg is not completed in one step; it is a gradual reduction from the higher valence Ti to monolithic titanium ($TiO_2 \rightarrow Ti_4O_7 \rightarrow Ti_3O_5 \rightarrow Ti_2O_3 \rightarrow TiO \rightarrow Ti$). Combining this fact with Table 1 shows that the ΔG_f^{Θ} of TiO is the largest, indicating that this aspect of the reduction of TiO to Ti is more difficult compared with other titanium oxides. Figure 1 also shows that the reduction of TiO_2 by Mg is accompanied by the formation of several intermediate compounds (such as $MgTiO_3$ and $MgTi_2O_5$). The results of the thermodynamic calculations using Eq. (1) indicate that it is feasible to reduce TiO_2 to Ti when sufficient Mg is present in the system (i.e., a_{Mg}=1):

$$TiO_2(s)+2Mg(s)=2MgO(s)+Ti(s) \quad (1)$$

Table 3 shows the $\Delta G_{f,i}^{\Theta}$ values of the compounds in the M−Cl−O system (M=Y, Mg) which were used in this study [27,28].

When $p_{O^{2-}}$ is defined as $\lg a_{O^{2-}}$, $\Delta G_{f,O^{2-}}^{\Theta}$ and $\Delta G_{f,Cl^-}^{\Theta}$ are zero. The electric potential–oxygen potential ($\varphi-p_{O^{2-}}$) diagram of the M−Cl−O (M=Mg, Y) system at different temperatures was calculated using the data presented in Table 3, Eqs. (2)−(4), and the Nernst equation (Eq. (5)), as shown in Fig. 2. Because the method of calculating $\varphi-p_{O^{2-}}$ plots is reported in the literature [29,30], only a brief overview is provided.

$$1/2O_2(s)+2e=O^{2-}\ (\text{in flux}) \quad (2)$$

$$Mg^{2+}(\text{in flux})+2e=Mg(l) \quad (3)$$

$$xO^{2-}(\text{in flux})+C(s)=CO_x(g)+2xe \quad (4)$$

$$\Delta G_r^{\Theta}=-zF\varphi \quad (5)$$

In Eq. (5), z is the number of electrons transferred during the chemical reaction, F= 96485 C/mol, and φ is the electrode potential (V).

Figure 2 shows that the oxygen content in Ti significantly decreases at an $Mg/MgCl_2$ equilibrium when the $a_{O^{2-}}$ ($a_{O^{2-}} \approx a_{MgO}$) value of the system is reduced (i.e., $p_{O^{2-}}$ increases). The Point X indicates that the concentration of oxygen in the Ti cannot be reduced below 19000×10^{-6} (a_{Mg}, a_{MgO} and a_{MgCl_2} equal 1, and $p_{O^{2-}}$ is 1.93 at 1173 K) even if the $p_{O^{2-}}$ decreases. Figure 2 shows that the electrode

Table 3 Standard Gibbs energy of formation for some compounds in M−O−Cl (M=Y, Mg) systems, and standard Gibbs energy of oxygen dissolution in β-Ti

Compound	ΔG_f^{Θ}/(J·mol^{-1})	T/K	ΔG_f^{Θ}(1073 K)/(J·mol^{-1})	ΔG_f^{Θ}(1173 K)/(J·mol^{-1})
Y_2O_3 (s)	$\Delta G_f^{\Theta}=-1895160+280.60T$	900−1200	−1594080	−1566020
YCl_3 (l)	$\Delta G_f^{\Theta}=-950725+183.52T$	994−1200	−753810	−735460
YOCl (s)	$\Delta G_f^{\Theta}=-1075000+219.50T$	1248−1375	−839480	−817530
MgO (s)	$\Delta G_f^{\Theta}=-608700+115.9T$	900−1200	−484340	−472750
MgO (l)	$\Delta G_f^{\Theta}=-539900+94.1T$	1100−1361	−438930	−429520
$MgCl_2$ (l)	$\Delta G_f^{\Theta}=-595315+112.81T$	987−1200	−474270	−462990
CO (g)	$\Delta G_f^{\Theta}=-114000-\times86.6T$	1100−1500	−206922	−215580
CO_2 (g)	$\Delta G_f^{\Theta}=-395000-\times0.651T$	1100−1500	−395700	−395760
[O] in Ti[a]	$\Delta G_f^{\Theta}=-583000+88.5T$	1173−1373	−488040	−479190
O^{2-} (in flux)[b]	$\Delta G_f^{\Theta}=53000-16.7T$	1100−1361	35080	33410

[a]: 1/2 O_2 (g) = [O] in Ti (1 wt.%), Henrian's 1 wt.% standard; [b]: 1/2 O_2 (g) + 2e = O^{2-}(in flux), molten salt is $MgCl_2$ (l)

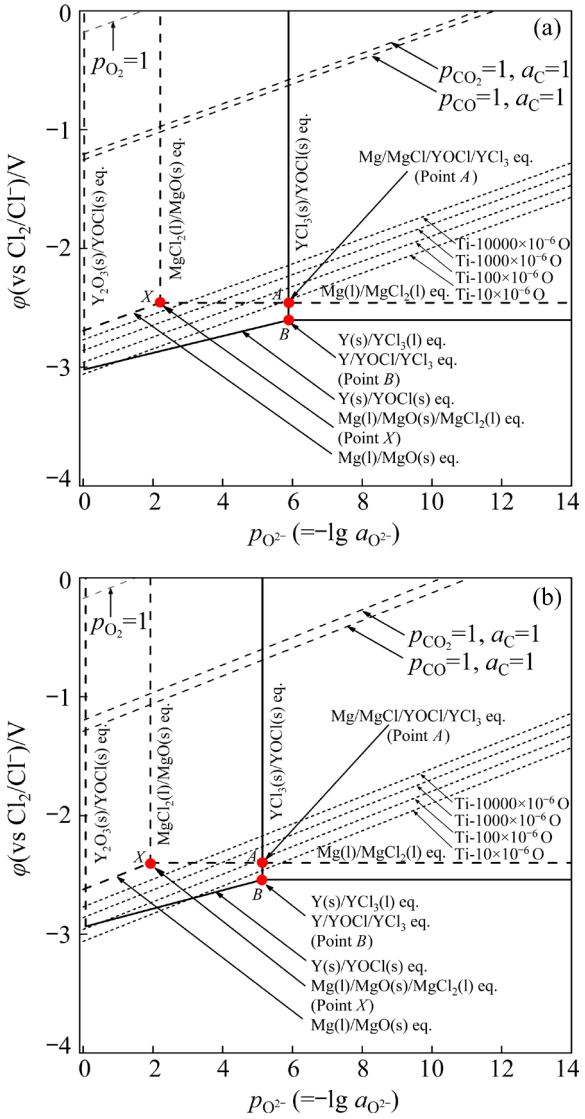

Fig. 2 φ−$p_{O^{2-}}$ diagrams of M−O−Cl system (M=Y, Mg) at different temperatures: (a) 1073 K; (b) 1173 K

potential of $MgCl_2$ (−2.46 V and −2.40 V at 1073 K) are higher than those of YCl_3 (−2.60 V and −2.54 V at 1173 K). When electrochemical deoxidation is performed in the $MgCl_2$−YCl_3 molten salt, magnesium metal is generated and deposited at the cathode as a reducing agent and deoxidizer. In addition, the reduction and deoxidation by-product, MgO, reacts with YCl_3 in the molten salt to form a YOCl precipitate, as shown in our previous studies [31]. However, Fig. 2 clearly shows that $a_{O^{2-}}$ significantly decreases and $p_{O^{2-}}$ rapidly increases to a value greater than 5 owing to the formation of YOCl. CO_x gas was also generated at the carbon anode. The results show that, because of YOCl precipitation and the simultaneous generation of CO_2 or CO gas, the Mg obtained by the in-situ electrolysis can effectively reduce the O content of Ti to less than 10×10^{-6}. Figure 2(a) confirms the feasibility of electrochemical reductive deoxidation in $MgCl_2$− YCl_3 molten salts.

3 Experimental

3.1 Materials

Table 4 lists characteristics of the raw material. The heating equipment used for this experiment consisted of a self-designed, highly-resistant furnace. A stainless steel reaction tank was used, and the electrochemical workstation was a CHI760E double constant potential instrument. In addition, a vacuum pump, filter, and tail gas treatment device were used, along with high-purity argon (99.99%).

Table 4 Characteristics of materials used for experiments

Material	Form	Purity/Grade	Supplier/Note
TiO_2	Powder	≥99.9%	Panzhihua Steel Titanium Industry Co., Ltd.
Ti crucible	89 mm in diameter, 3 mm in thickness, and 350 mm in height	CP-Ti[a]	Baoji Chenhui Metal Materials Co., Ltd.
Ti foil	0.2 mm in thickness	CP-Ti[a]	Baoji Chenhui Metal Materials Co., Ltd.
Ti-wire	2.0 mm in diameter	1200×10^{-6}	Baoji Chenhui Metal Materials Co., Ltd.
Ti sponges	Sponge	≥97.0%	Panzhihua Steel Titanium Industry Co., Ltd.
Anhydrous $MgCl_2$	Powder	99.9%	Aladdin reagent
Anhydrous KCl	Powder	99.0%	Aladdin reagent
Anhydrous YCl_3	Powder	99.9%	Aladdin reagent
Anhydrous $CaCl_2$	Powder	99.99%	Aladdin reagent
Y	Shot	99.9%	Aladdin reagent

[a]: CP-Ti: Commercially-pure titanium with 95% titanium

3.2 Setup and procedure

Figure 3 is a schematic of the experimental setup for the electrochemical reduction of TiO_2 in the molten salt of $MgCl_2$−10mol.%YCl_3 or $MgCl_2$−10mol.%YCl_3−10mol.%KCl. TiO_2 was used as the experimental feedstock, and electrochemical reduction experiments were performed in a high-purity Ar atmosphere. The electrodes and thermocouples were inserted from the top. In addition, the electrochemical deoxidation experiments were performed in the same molten salt using a Ti wire with an initial oxygen content of 1200×10^{-6} as the raw material to verify the limits of electrochemical deoxidation in the system.

First, anhydrous $MgCl_2$ and KCl powders, and yttrium (Y) were weighed and used to produce YCl_3 via the chemical reaction shown in Eq. (6), thereby producing $MgCl_2$−YCl_3 and $MgCl_2$−YCl_3−KCl molten salts with different compositions.

$$Y(s)+3/2MgCl_2(l)=3/2Mg(l)+YCl_3(l) \quad (6)$$

Next, $MgCl_2$ and KCl powders were vacuum-dried at 473 K for 48 h and then transferred to a Ti crucible containing metallic Y and Ag (60 g). To prepare the Y- or Ag-containing titanium crucible, a C rod, Ti, Ni, and Mo wire was first inserted into one end of a stainless steel tube and fastened with a short screw. Subsequently, a Ni wire with a diameter of 5 mm, working as the lead, was passed through an alumina protective sleeve, then through a steel tube, and wrapped around the screw. Then, the Ti crucible was positioned in a stainless steel reaction vessel. Some alumina balls were placed at the bottom of the stainless steel reactor in advance to prevent the Ti crucible and stainless steel from adhering. The prepared electrode and thermocouple were inserted into the top lid of the reactor, while their other ends were sealed with rubber plugs. Furthermore, the system pressure was reduced to less than 10 Pa by turning on the vacuum pump. The temperature was set to 673 K for 48 h to completely remove the moisture from the molten salt. After vacuum drying, the glass valve of the vacuum pump was closed and filled with Ar gas. When the pressure reached a slightly positive value, the outlet valve was opened to prevent reverse suction.

The temperature increased to the level required for this study, and cyclic voltammetry (CV) was performed. The electrodes used for the CV tests included *d*2 mm-C, *d*3 mm-Ni, and *d*1 mm-Mo electrodes. After the CV tests, the flux was electrolyzed for up to 48 h, with the *d*6 mm-C electrode as the anode and Mo as the cathode. After electrolysis, the *d*6 mm C-electrode was used as the anode, an electrode containing TiO_2 was used as the cathode, and the electrolysis experiment was then conducted according to the amperometric *I*−*t* curve method.

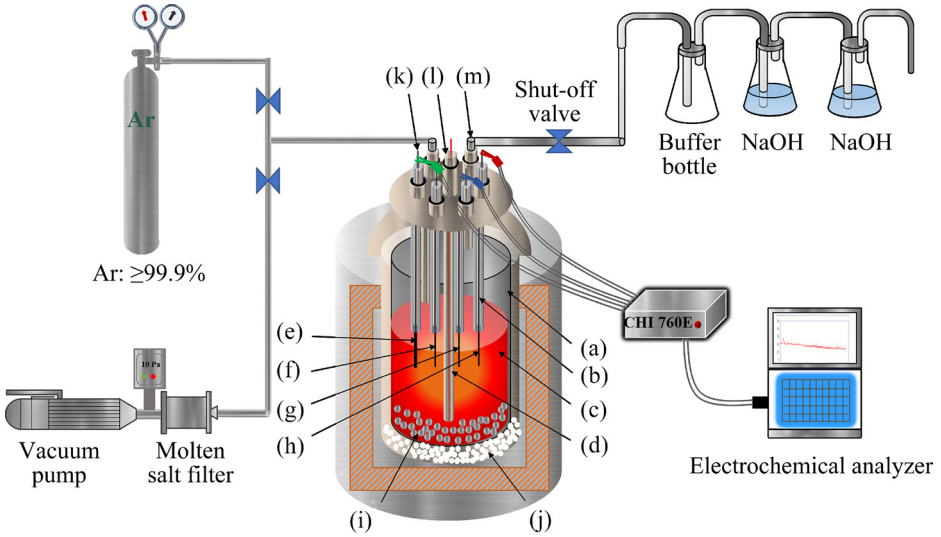

Fig. 3 Schematic of experimental setup for electrochemical reduction of TiO_2 in $MgCl_2$−10mol.%YCl_3 or $MgCl_2$−10mol.%YCl_3−10mol.%KCl molten salt: (a) Ti crucible; (b) Al_2O_3 insulation tube; (c) $MgCl_2$−YCl_3 molten salt or $MgCl_2$−YCl_3−KCl molten salt; (d) Thermocouple; (e) Graphite anode (*d*6 mm (or *d*2 mm, for CV test)); (f) Ni electrode (*d*3 mm, for CV test); (g) Mo electrode (*d*1 mm); (h) TiO_2 cathode; (i) Ag shot; (j) Alumina balls; (k) Ni wire (potential lead); (l) Stainless steel tube (current lead); (m) Rubber plug

3.3 Product testing method

The TiO_2 electrolytic reduction products were washed with hydrochloric acid (2 mol/L) and distilled water and dried under vacuum conditions. X-ray diffraction (XRD) was used to determine the phase composition of the reduction products. Scanning electron microscopy (SEM) was used to observe the morphology of the reduction products and energy-dispersive X-ray spectroscopy (EDS) was used to analyze the elemental species and content of the microregions. Because the molten salts and by-product (YOCl) of deoxidation remained on the surface of the Ti specimens, the Ti specimens were chemically etched using a mixture of $HF-HNO_3-H_2O$ (1:4:10), rinsed with distilled water, and dried. Finally, the Ti samples were tested for their oxygen content with a LECO TC−400 instrument.

4 Results and discussion

4.1 Molten salt electrolysis−magnesiothermic reduction of TiO_2 in $MgCl_2-YCl_3$ molten salt

Figure 4 shows the CV curves of the $MgCl_2$−10mol%YCl_3 flux at 1073 K. An oxidation peak appears at ~1.7 V, which represents the precipitation of the oxygen ions (O^{2-}) and the escape of gas in the system. This is indicative of Eq. (4), that is, CO and CO_2 are produced in the system. An oxidation peak also appears at 2.4 V, which corresponds to the settling of Cl^-. The applied voltage was maintained above 2.4 V during the electrolysis to produce the reductant Mg required for reducing TiO_2.

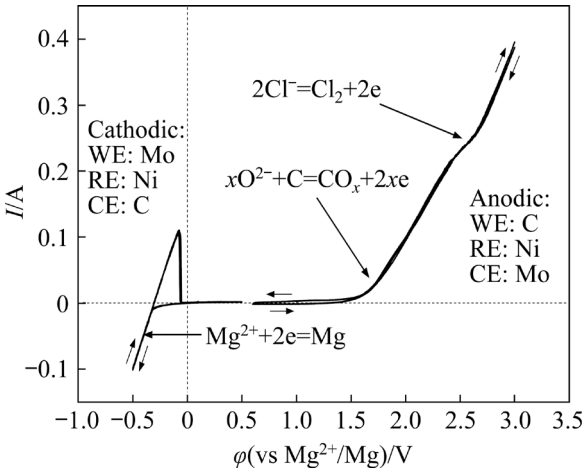

Fig. 4 CV curve of $MgCl_2$−10mol.%YCl_3 molten salt at 1073 K (electrode contact area: ~20 mm^2)

In this study, TiO_2 powder was pressed into the shape of a 13 mm-diameter flake at 227 MPa and sintered at 1273 K for 12 h to facilitate the collection of the Ti generated after the electrochemical reduction. Figure 5 shows the XRD pattern of raw TiO_2 and a photograph of a flake after pressing. Table 5 shows the experimental conditions employed in this study. Figure 6 shows the XRD patterns of the products after the experiments at different applied voltages and electrolysis time at 1073 K. Figure 7 shows the XRD patterns of the products after the experiment at 1173 K at different applied voltages and electrolysis time.

Table 5 Experimental conditions for electrolytic reduction of TiO_2 in $MgCl_2-YCl_3$ flux

No.	Composition	T/K	U/V	t/h	m_{TiO_2}/g
#1-1	$MgCl_2$−10mol.%YCl_3	1073	2.9	25	0.23
#1-2	$MgCl_2$−10mol.%YCl_3	1073	2.7	36	0.23
#1-3	$MgCl_2$−10mol.%YCl_3	1073	2.6	25	0.23
#1-4	$MgCl_2$−10mol.%YCl_3	1073	2.6	36	0.23
#1-5	$MgCl_2$−30 mol.% YCl_3	1173	3.1	24	0.23
#1-6	$MgCl_2$−30 mol.% YCl_3	1173	2.5	24	0.23
#1-7	$MgCl_2$−30 mol.% YCl_3	1173	2.6	36	0.23
#1-8	$MgCl_2$−30 mol.% YCl_3	1173	2.5	36	0.23

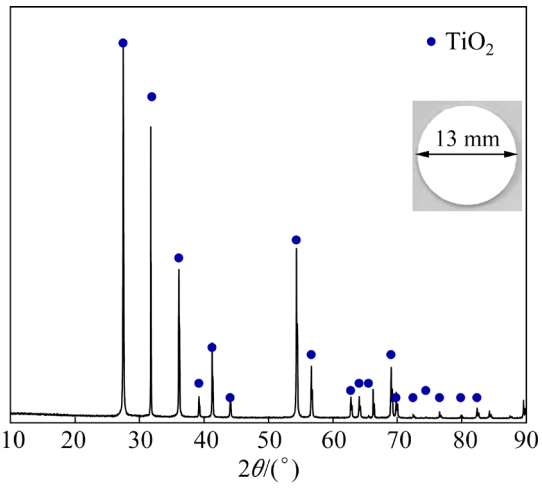

Fig. 5 XRD pattern of product

Table 5 and Figs. 6 and 7 show that by maintaining the applied voltage between 2.5 and 3.1 V and the electrolysis time between 24 and 36 h, Mg reduces TiO_2 to Ti_3O_5, Ti_2O_3, and other compounds. This yields Ti_3O and Ti_6O as high-oxygen Ti, accompanied by the generation of YOCl.

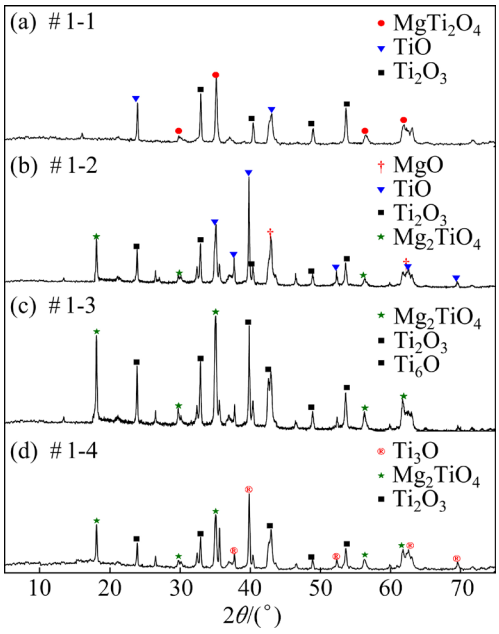

Fig. 6 XRD patterns for products obtained after experiments with different voltages and time at 1073 K

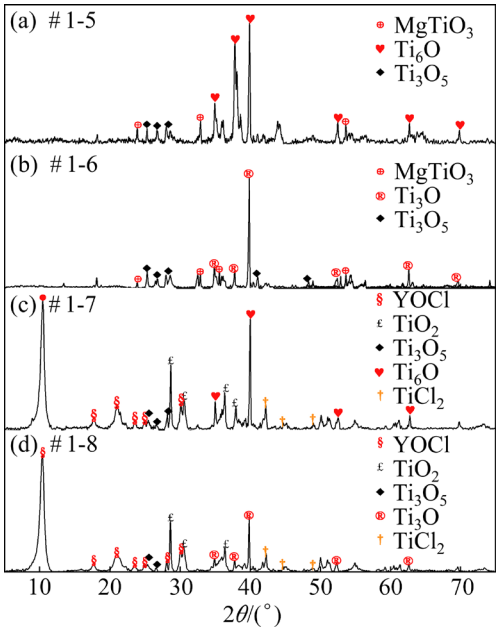

Fig. 7 XRD patterns for products obtained with different voltages and time at 1173 K

Combining these findings with the data provided in Table 5 and Figs. 6 and 7, it is observed that changing the temperature from 1073 to 1173 K increases the diffusion rate of ions in the system. It also increases the YCl_3 content (from 10 to 30 mol.%), effectively reducing the O^{2-} concentration in the system because YOCl is generated (Eq. (7)). By further increasing the electrolytic time (experiments #1-3, #1-4, #1-7, #1-6 and #1-8, using the same applied voltage and increasing the electrolytic time), only Ti_6O was obtained.

$$MgO(s)+YCl_3(l)=MgCl_2(l)+YOCl(s) \quad (7)$$

This result may be attributed to the following reasons: (1) MgO generated through the reaction hindered the reduction of TiO_2 by Mg (MgO was not detected because the electrolysis products in this study were all cleaned with hydrochloric acid); (2) Because the density of Mg was lower than that of the molten salt, the reductant Mg generated via electrolysis floated on the upper surface of the molten salt, resulting in an incomplete reduction; (3) The raw TiO_2 material was very dense because it was pre-pressed and sintered. Therefore, the internal oxygen ions could not be effectively removed, i.e., the transfer efficiency was very low, thereby resulting in an incomplete reduction reaction.

4.2 Molten salt electrolysis−magnesiothermic reduction of TiO_2 preform in $MgCl_2$−YCl_3 molten salt

SUZUKI and INOUE [32], OKABE et al [33], and LEI et al [34] have reported efficient calciothermic reduction of preforms containing $CaTiO_3$ prepared by adding $CaCl_2$ to TiO_2. In this study, sintered preforms were obtained by adding 10mol.%$CaCl_2$ to TiO_2. Next, $CaCl_2$, TiO_2, and water were mixed and placed in a pre-made mold and sintered in a muffle furnace at 1273 K for 2 h. Figure 8 shows the photograph and XRD pattern of the preform after sintering. Figure 9 shows the SEM-EDS analyses of the raw titanium dioxide without $CaCl_2$ and the sintered preforms.

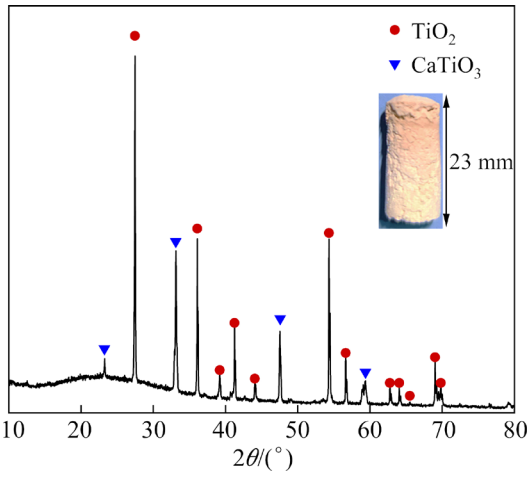

Fig. 8 XRD pattern and photograph of sintered preform

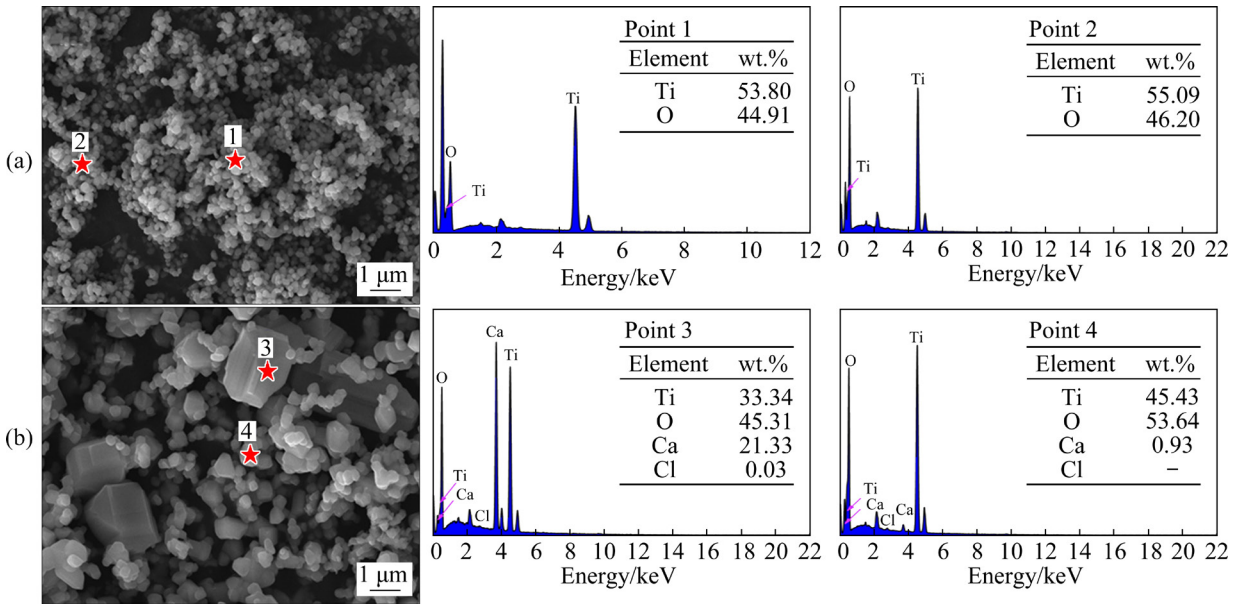

Fig. 9 SEM-EDS analyses of raw materials: (a) TiO_2 (without $CaCl_2$); (b) Preform

Figure 9 shows that the sintered preforms have a higher $CaTiO_3$ contents in the physical phase composition compared with TiO_2 (Fig. 5). In addition, combined with the SEM-EDS results, clearly, titanium obtained had a porous structure because the generation of $CaTiO_3$ increased the porosity of the TiO_2 feedstock.

Figure 10 shows the CV curves of $MgCl_2$–10mol.%YCl_3–10mol.%KCl at 1173 K. The oxidation peaks of O^{2-} and Cl^- at 1173 K (1.9 and 2.5 V) are shifted to the right compared to those at 1073 K (1.7 and 2.4 V), and the increase in ΔG_r^{Θ} at the higher temperature leads to an increase in the electrode potential, as shown in Eq. (5).

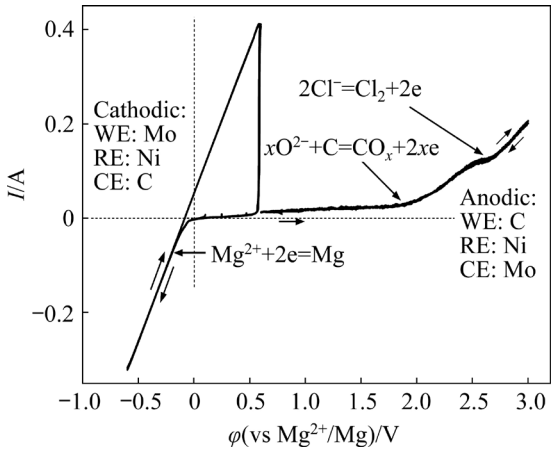

Fig. 10 CV curves of $MgCl_2$–10mol.%YCl_3–10mol.%KCl molten salt at 1173 K (electrode contact area: ~20 mm^2)

Table 6 lists the experimental conditions used in this study. Figure 11 shows the XRD patterns and photograph of the electrolytic reduction product. Note that this electrolysis product was washed with water.

Table 6 Experimental conditions for electrolytic reduction of preform in $MgCl_2$–YCl_3–KCl flux

No.	Composition	T/K	U/V	t/h	$m_{preform}$/g
#2-1	$MgCl_2$–10mol.%YCl_3–10mol.%KCl	1173	2.6	48	1.50
#2-2	$MgCl_2$–10mol.%YCl_3–10mol.%KCl	1173	2.5	48	1.50
#2-3	$MgCl_2$–10mol.%YCl_3–10mol.%KCl	1173	2.7	48	1.50
#2-4	$MgCl_2$–30mol.%YCl_3–10mol.%KCl	1173	2.6	48	1.50

As shown in Fig. 11, the electrolysis products after geometrically increasing the mass of the feedstock are Ti_2O, Ti_3O, and Ti_6O, along with high-oxygen content Ti. This indicates that the production of the Mg reducing agent during the electrolysis of $MgCl_2$ is not a limiting factor in the incomplete reduction of the TiO_2. Comparing the data in Figs. 6 and 11, the reduction is more effective for the preforms prepared by adding $CaCl_2$ as a melting agent (#2-2 and #2-3) compared with those without $CaCl_2$ (#1-2 and #1-3). The effect of the YCl_3 content on the reduction is also less clear

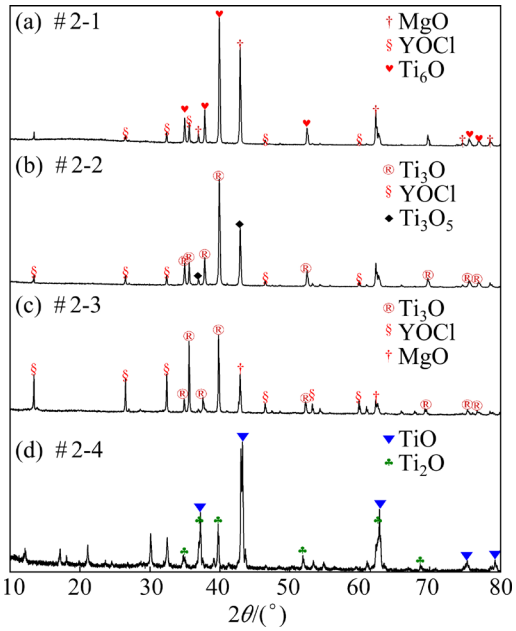

Fig. 11 XRD patterns of products obtained after electrolytic reduction

in Fig. 11(d) (#2-4) compared with Fig. 11(a) (#2-1). The exterior and interior of the #2-1 product were separately analyzed using SEM-EDS. The results (Fig. 12 and Table 7) further verify that the reduction of TiO_2 by Mg is feasible (Fig. 1).

Figure 12 and Table 7 show that Ti and O are mainly present on the outer surface of the electrolysis product #2-1, with the highest and lowest titanium content being 94.31% and 90.35%, respectively, indicating that high-purity Ti metal was present. The inside of the electrolysis product #2-1, which was attached to the surface by a considerable amount of MgO, is shown in Figs. 12 (c) and (d). These figures need to be considered in combination with Fig. 11(a). The MgO failed to react with YCl_3 to form YOCl in a timely fashion. It also hindered the magnesiothermic reduction of TiO_2, resulting in a high volume of Ti−O in the incomplete reduction product.

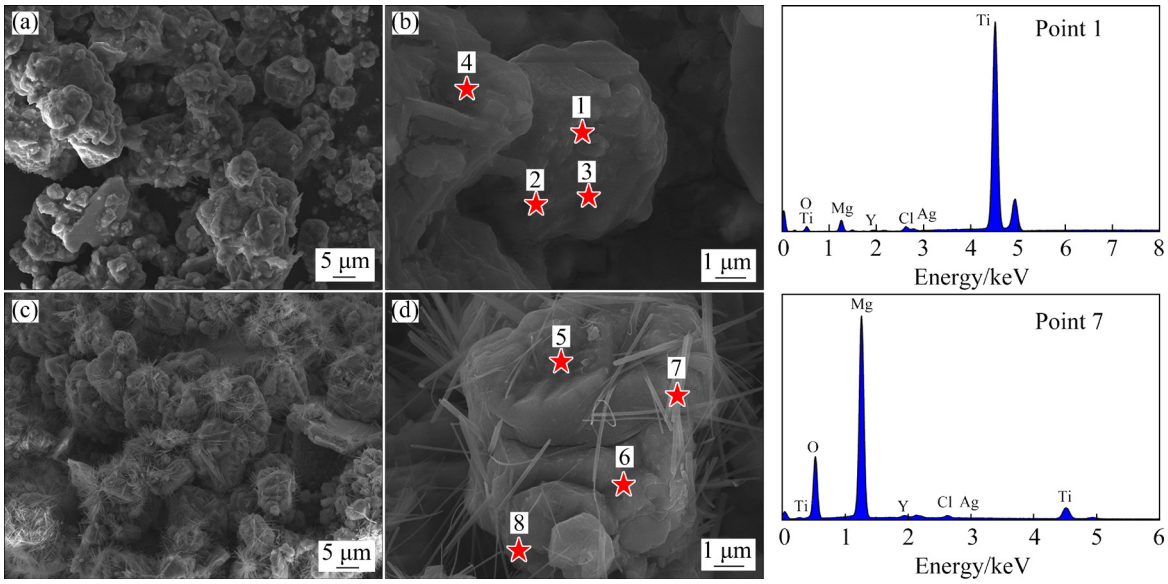

Fig. 12 SEM-EDS results of #2-1 product: (a) Exterior (5 μm); (b) Exterior (1 μm); (c) Interior (5 μm); (d) Interior (1 μm)

Table 7 Composition of surface of product analyzed using EDS (wt.%)

Product parts	Point	Ti	Mg	Y	Ag	O	Cl
Exterior	1	90.35	1.95	0.40	0.03	6.55	0.72
	2	91.86	1.53	0.41	0.00	5.5	0.70
	3	94.31	0.87	0.04	0.00	4.69	0.10
	4	92.80	1.59	0.00	0.20	5.31	0.10
Interior	5	48.74	19.08	1.92	0.01	29.38	0.87
	6	58.10	14.23	0.12	0.10	25.21	1.09
	7	10.27	45.56	1.66	0.04	38.48	0.99
	8	71.50	8.50	1.68	0.00	17.22	1.10

4.3 Deoxidation of high-oxygen Ti in $MgCl_2$–YCl_3 molten salt

Deoxidation is required to reduce the oxygen content of the high-oxygen Ti obtained from the direct reduction of TiO_2. This study used the $MgCl_2$−10mol.%YCl_3 flux and Ti wire with an oxygen content of 1200×10^{-6} as the raw material. Table 8 shows the experimental conditions and results.

Table 8 Experimental conditions and results of electrochemical deoxidation

No.	Composition	T/K	U/V	t/h	Oxygen content/10^{-6}	
					Initial	After
#3-1	$MgCl_2$–10mol.%YCl_3	1173	2.5	24	1200	27
#3-2	$MgCl_2$–10mol.%YCl_3	1173	2.5	20	1200	73

Table 8 shows that the oxygen content in titanium could be reduced from 1200×10^{-6} to less than 100×10^{-6} or even to 27×10^{-6}, by applying a voltage of 2.5 V at 1173 K. The results show that with the help of YOCl precipitation and simultaneous CO_x generation in the $MgCl_2$–YCl_3 system, Mg generated by electrolysis could effectively reduce the solid-dissolved oxygen content in a considerable amount of Ti metal to less than 100×10^{-6}. The results of the φ–$p_{O^{2-}}$ diagram of the M−Cl−O (M=Mg,Y) system representing the thermodynamic theory (Fig. 2) were also validated. This study will aid in the production of ultra-low-oxygen metallic Ti powders from high-oxygen Ti obtained via the electrolytic reduction of TiO_2. Compared with the FFC, OS and other deoxygenation methods, the deoxidation limit of the proposed method is very low. Furthermore, this process is environmentally friendly with no waste water or gas generation.

4.4 Presentation of new technology

This study proposes a sustainable, environmentally-friendly molten salt electrolysis–magnesiothermic reduction process for TiO_2 to produce ultralow-oxygen metallic Ti powder (Fig. 13), which uses the results of the theoretical and experimental studies as a foundation. In this process TiO_2 can be directly used as a raw material. After high-oxygen content Ti was obtained through electrolytic reduction, electrochemical deoxidation was conducted to obtain ultralow-oxygen Ti with an oxygen content below 100×10^{-6}. This electrolytic deoxidation can be directly used to recycle high-oxygen content Ti scrap. Vacuum distillation could efficiently remove the molten salts, such as $MgCl_2$, which remain on the surface of the titanium powder after reduction and deoxidation; the waste gas, waste water and industrial residue were not generated. Finally, the reduction and deoxidation

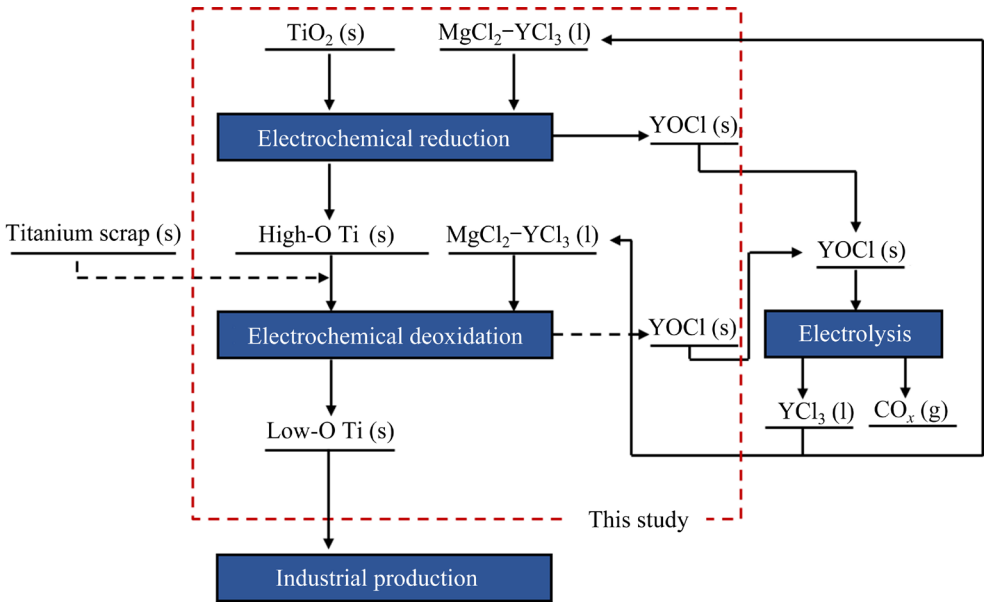

Fig. 13 Sustainable process for recycling of Ti scrap and clean and efficient preparation of low-oxygen Ti via direct reduction of TiO_2

by-product, YOCl, could be recycled using electrolysis to produce YCl_3, which could be reused as electrolytic feedstock for reduction and deoxidation during the entire process, thereby realizing the recycling of the by-products without requiring new materials.

5 Conclusions

(1) The calculated Mg−Ti−O phase diagram shows that the reduction of TiO_2 by magnesium is feasible; the calculated $\varphi-p_{O^{2-}}$ diagrams show that the generation of YOCl can effectively reduce the O^{2-} concentration in the system; and the deoxygenation effect is significant.

(2) The experimental results show that TiO_2 was reduced to Ti−O compounds or high-oxygen Ti (Ti_6O) by electrochemical reduction at 1073−1173 K under an applied voltage of 2.5−3.1 V. In addition, the reason for the incomplete reduction of TiO_2 in the $MgCl_2$−YCl_3 and $MgCl_2$−YCl_3−KCl molten salts was determined.

(3) The obtained high-oxygen Ti was electrochemically deoxidized in the same system, and its oxygen content was reduced from 1200×10^{-6} to less than 100×10^{-6}.

(4) A sustainable, clean, and efficient processes are proposed for the industrial production of low-oxygen Ti by the direct reduction of TiO_2 and for recycling high-oxygen Ti scrap.

CRediT authorship contribution statement

Jian PANG: Conceptualization, Methodology, Investigation, Writing − Original draft, Review & editing; **Ling-xin KONG:** Conceptualization & methodology; **Li-guo ZHU:** Methodology & investigation; **Bao-qiang XU:** Investigation; **Jun-jie XU:** Investigation; **Chong-lin BAI:** Investigation; **Bin YANG:** Conceptualization and methodology.

Declaration of competing interest

The authors declare that they have no competing financial interests or personal relationships that may have influenced the work reported in this study.

Acknowledgments

The authors are grateful for the financial support provided by the National Natural Science Foundation of China (No. 21968013), Fundamental Research Project of Yunnan Province, China (No. 202201AT070229), and Kunming University of Technology High-level Talent Platform Construction Project of Science and Technology, China (No. KKKP201752023).

References

[1] REN Li-rong, QIN Shui-jie, ZHAO Si-hao, XIAO Hua-qiang. Fabrication and mechanical properties of Ti_2AlC/TiAl composites with co-continuous network structure [J]. Transactions of Nonferrous Metals Society of China, 2021, 31(7): 2005−2012.

[2] WANG Wen-chang, LI Jia-xing, GE Yuan, KONG De-jun. Structural characteristics and high-temperature tribological behaviors of laser cladded NiCoCrAlY−B_4C composite coatings on Ti_6Al_4V alloy [J]. Transactions of Nonferrous Metals Society of China, 2021, 31(9): 2729−2739.

[3] MIHALCEA E, VERGARA-HERNÁ NDEZ H J, JIMENEZ O, OLMOS L, CHÁVEZ J, ARTEAGA D. Design and characterization of Ti_6Al_4V/20CoCrMo−highly porous Ti_6Al_4V biomedical bilayer processed by powder metallurgy [J]. Transactions of Nonferrous Metals Society of China, 2021, 31(1): 178−192.

[4] BARTOLOMEU F, BUCIUMEANU M, PINTO E, ALVES N, SILVA F S, CARVALHO O, MIRANDA G. Wear behavior of Ti_6Al_4V biomedical alloys processed by selective laser melting, hot pressing and conventional casting [J]. Transactions of Nonferrous Metals Society of China, 2017, 27(4): 829−838.

[5] GUPTA M K, SOOD P K, SHARMA V S. Investigations on surface roughness measurement in minimum quantity lubrication turning of titanium alloys using response surface methodology and box−cox transformation [J]. Journal for Manufacturing Science and Production, 2016, 16: 75−88.

[6] ZHOU Yang, YANG Fang, CHEN Cun-guang, SHAO Yan-ru, LU Bo-xin, LU Tian-xing, SUI Yan-li, GUO Zhi-meng. Mechanical property enhancement of high-plasticity powder metallurgy titanium with a high oxygen concentration [J]. Journal of Alloys and Compounds, 2021, 885: 161006.

[7] TAKEDA O, OKABE T H. Current status of titanium recycling and related technologies [J]. JOM, 2019, 71: 1981−1990.

[8] YAO Wen-jing. Major foreign commercial aviation markets and their titanium consumption in 2020 [J]. China Metal Bulletin, 2021(9): 7−9. (in Chinese)

[9] ZHANG Ce. Study on loe interstitials titanium alloy prepared by reaction synthesis from HDH titanium powder [D]. Beijing: University of Science and Technology Beijing, 2019: 1−140. (in Chinese)

[10] AN Zhong-sheng, CHEN Yan, ZHAO Wei. Report on China titanium industry progress in 2021 [J]. Titanium Industry Progress, 2022, 39(4): 34−43. (in Chinese)

[11] QIU Guan-zhou, GUO Yu-feng. Current situation and development trend of titanium metal industry in China [J]. International Journal of Minerals, Metallurgy and Materials, 2022, 29(4): 599−610.

[12] LIU Mei-feng, LU Shi-guang, KAN Su-rong, LI Guo-xun. Effect of electrolysis voltage on electrochemical reduction of titanium oxide to titanium in molten calcium chloride [J]. Rare Metals, 2007, 26(6): 547−551.

[13] CHEN G Z, FRAY D J, FARTHING T W. Direct electrochemical reduction of titanium dioxide to titanium in molten calcium chloride [J]. Nature, 2000, 407: 361−364.

[14] ONO K, SUZUKI R O. A new concept for producing Ti sponge: Calciothermic reduction [J]. JOM, 2002, 54(2): 59−61.

[15] ZHU Hong-min, JIAO Shu-qiang. GU Xue-fan. A method for the electrolytic production of pure titanium from titanium monoxide/titanium carbide soluble solid solution anodes [P]. China Patent: CN1712571, 2015. (in Chinese)

[16] GARDARELLI F. Method for electrowinning of titanium metal or alloy from titanium oxide containing compound in the liquid state: US Patent [P]. 7504017B2, 2009.

[17] SUPUT M, DELUCAS R, PATI S, YE G, PAL U, POWELL A C. Solid oxide membrane technology for environmentally sound production of titanium [J]. Mineral Processing and Extractive Metallurgy, 2008, 117(2): 118−122.

[18] CHEN G Z, FRAY D J, FARTHING T W. Cathodic deoxygenation of the alpha case on titanium and alloys in molten calcium chloride [J]. Metallurgical and Materials Transactions B, 2001, 32(6): 1041−1052.

[19] XIA Yang, FANG Zhi-gang, SUN Pei, ZHANG Ying, ZHANG Tuo-yang, FREE M. The effect of molten salt on oxygen removal from titanium and its alloys using calcium [J]. Journal of Materials Science, 2017, 52: 4120−4128.

[20] ZHANG Ying, FANG Zhi-gang, SUN Pei, ZHANG Tuo-yang, XIA Yang, ZHOU Cheng-shaung, HUANG Zhe. Thermodynamic destabilization of Ti−O solid solution by H_2 and deoxygenation of Ti using Mg [J]. Journal of the American Chemical Society, 2016, 138: 6916−6919.

[21] MOON B M, SEO J H, LEE H J, JUNG K H, PARK J H, JUNG H D. Method of recycling titanium scraps via the electromagnetic cold crucible technique coupled with calcium treatment [J]. Journal of Alloys and Compounds, 2017, 727: 931−939.

[22] OKABE T H, NAKAMURA M, OISHI T, ONO K. Electrochemical deoxidation of titanium [J]. Metallurgical and Materials Transactions B, 1993, 24(3): 449−455.

[23] TANINOUCHI Y K, HAMANAKA Y, OKABE T H. Electrochemical deoxidation of Titanium and its alloy using molten magnesium chloride [J]. Metallurgical and Materials Transactions B, 2016, 47(6): 3394−3404.

[24] OKABE T H, HAMANAKA Y, TANINOUCHI Y K. Direct oxygen removal technique for recycling titanium using molten $MgCl_2$ salt [J]. Faraday Discussions, 2016, 190: 109−126.

[25] ZHENG C Y, OUCHI T, IIZUKA A, TANINOUCHI Y K, OKABE T H. Deoxidation of titanium using Mg as deoxidant in $MgCl_2$−YCl_3 flux [J]. Metallurgical and Materials Transactions B, 2019, 50(2): 622−631.

[26] BARIN I. Thermochemical data of pure substances [M]. 3rd Edition. Wiley-VCH, Germany: Verlagsgesellschaf mbH Press.

[27] OKABE T H, ZHENG C Y, TANINOUCHI Y K. Thermodynamic considerations of direct oxygen removal from titanium by utilizing the deoxidation capability of rare earth metals [J]. Metallurgical and Materials Transactions B, 2018, 49(3): 1056−1066.

[28] ZHENG C Y, OUCHI T, KONG L X, TANINOUCHI Y K, OKABE T H. Electrochemical deoxidation of titanium in molten $MgCl_2$−YCl_3 [J]. Metallurgical and Materials Transactions B, 2019, 50(4): 1652−1661.

[29] KONG L X, OUCHI T, ZHENG C Y, OKABE T H. Electrochemical deoxidation of Titanium scrap in $MgCl_2$−$HoCl_3$ system [J]. Journal of the Electrochemical Society, 2019, 166(13): E429−E437.

[30] LITTLEWOOD R. Diagrammatic representation of the thermodynamics of metal-fused chloride systems [J]. Journal of the Electrochemical Society Absorbed Electrochem Technol, 1962, 109(6): 525.

[31] PANG Jian, KONG Ling-xin, XU Jun-jie, YOU Yan-jun, XU Bao-qiang, YANG Bin. Study on the direct deoxidation of solid dissolved oxygen with Titanium using Mg in $MgCl_2$−YCl_3 flux [J]. Nonferrous Metals Engineering, 2022, 12(2): 67−74. (in Chinese)

[32] SUZUKI R O, INOUE S. Calciothermic reduction of titanium oxide in molten $CaCl_2$ [J]. Metallurgical and Materials Transactions B, 2003, 34(3): 277−285.

[33] OKABE T H, ODA T, MITSUDA Y. Titanium powder production by preform reduction process (PRP) [J]. Journal of Alloys and Compounds, 2004, 364: 156−163.

[34] LEI Xian-jun, XU Bao-qiang, YANG Guo-bo, SHI Teng-teng, LIU Da-chun, YANG Bin. Direct calciothermic reduction of porous calcium titanate to porous titanium [J]. Materials Science and Engineering: C, 2018, 91: 125−134.

TiO_2直接还原制备超低氧钛

庞 佺[1,2,3]，孔令鑫[1,2,3,4]，朱立国[1,2,3]，徐宝强[1,2,3,4]，徐俊杰[1,2,3]，白崇霖[1,2,3]，杨 斌[1,2,3,4]

1. 昆明理工大学 云南省有色金属真空冶金重点实验室，昆明 650093；
2. 昆明理工大学 真空冶金国家工程研究中心，昆明 650093；
3. 昆明理工大学 冶金与能源工程学院，昆明 650093；
4. 昆明理工大学 省部共建复杂有色金属资源清洁利用国家重点实验室，昆明 650093

摘 要：提出在 $MgCl_2$−KCl−YCl_3 熔盐中，通过熔盐电解产生 Mg 直接还原 TiO_2 制备低氧钛。绘制 Mg−Ti−O 三元相图和电位−氧势(φ−$p_{O^{2-}}$)图，表明镁还原 TiO_2 制备低氧钛是可行的。在 $MgCl_2$−YCl_3 和 $MgCl_2$−YCl_3−KCl 熔盐中，不同温度和施加电压条件下，开展熔盐电解−镁热还原 TiO_2 实验研究，结果表明：借助 YOCl 沉淀及 CO_x 同步生成，将还原和脱氧产物 O^{2-}快速脱除，在 1073~1173 K、施加电压 2.5~3.1 V 的条件下，通过电化学还原可以将 TiO_2 还原为高氧钛(Ti_6O)。在温度为 1173 K 的 $MgCl_2$−YCl_3 熔盐中，开展不同施加电压下的高氧钛电化学脱氧实验。此外，还观察到有可能将高氧钛的氧含量可从 1200×10^{-6} 降至 100×10^{-6} 以下。

关键词：二氧化钛；电化学；镁热还原；脱氧；超低氧钛；稀土金属

(Edited by Xiang-qun LI)